

875 USGS-OFR-81-1336

UNITED STATES DEPARTMENT OF INTERIOR
GEOLOGICAL SURVEY

Interpretation of hole-to-surface resistivity measurements

at Yucca Mountain, Nevada Test Site

by

Jeffrey J. Daniels and James H. Scott

Open-File Report 81-1336

1981

This report is preliminary and has not been reviewed for conformity
with U.S. Geological Survey editorial standards.
Any use of trade names is for descriptive purposes only
and does not imply endorsement by the USGS.

Interpretation of hole-to-surface resistivity measurements
at Yucca Mountain, Nevada Test Site

by

Jeffrey J. Daniels and James H. Scott

Abstract

Hole-to-surface measurements from drill holes UE25a-1, -4, -5, and -6 illustrate procedures for gathering, reducing, and interpreting hole-to-surface resistivity data. The magnitude and direction of the total surface electric field resulting from a buried current source is calculated from orthogonal potential difference measurements for a grid of closely-spaced stations. A contour map of these data provides a detailed map of the distribution of the electric field away from the drill hole. Resistivity anomalies can be enhanced by calculating the difference between apparent resistivities calculated from the total surface electric field, and apparent resistivities for a layered earth model.

Lateral discontinuities in the geoelectric section are verified by repeating the surface field measurements for current sources in different drill holes. A qualitative interpretation of the anomalous bodies within a layered earth can be made by using a three dimensional resistivity model in a homogeneous half-space. The general nature of resistive and conductive bodies causing anomalies away from the source drill holes is determined with the aid of data from several source holes, layered models, and three dimensional models.

Hole-to-surface resistivity measurements at Yucca Mountain indicate the presence of many near-surface geologic inhomogeneities, with no definite indication of deep structural features. A resistive anomaly near drill hole UE25a-6 is interpreted as a thin, vertical, resistive body that nearly intersects the surface, and may be caused by a silicified, or calcified, fracture zone. A resistive anomaly near hole UE25a-7 is probably caused by a near surface, horizontal, lens-shaped body that may represent a devitrified zone in the Tiva Canyon Member. Many conductive anomalies were detected to the southwest of hole UE25a-4. However, these anomalies are interpreted to be caused by variations in the thickness of the surface alluvium.

Introduction

Hole-to-surface resistivity measurements are made by placing an electric current source in a drill hole and measuring the resulting distribution of electric potential on the earth's surface. *Mise a la masse* is a specialized version of the hole-to-surface resistivity measurement technique that utilizes a current electrode placed in a conductive body.

The field measurements presented in this paper are from drill holes UE25a-1, -4, -5, and -6, Yucca Mountain, Nevada Test Site. These holes, shown in figure 1, are located in a southeast trending valley, and penetrate a thick sequence of rhyolitic tuffs, that has been described by Spengler and others (1979) and Spengler and Rosenbaum (1980). The stratigraphic dip of the volcanic tuff sequence is approximately equal to the topographic dip along a line joining drill holes UE25a-1 and -4. Geophysical well logs for each of these drill holes have been presented by Hagstrum and others (1980) and Daniels and others (1981).

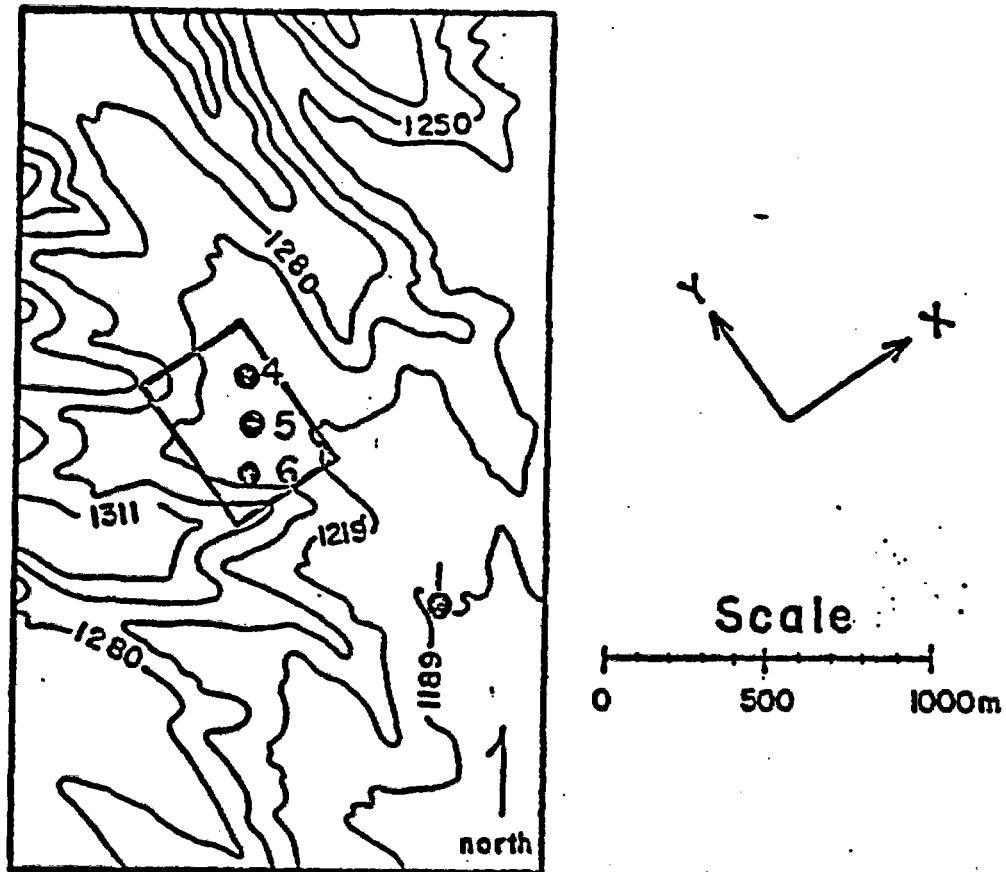


Figure 1.—Location map of electric current source holes (UE25a-1, -4, -5, and -6) used in this study. Topographic contours are in meters. The heavy line around the drill holes shows the region of gridded measurements discussed in the text and shown in subsequent figures.

Hole-to-surface resistivity field measurements

The primary requisite for a resistivity array is that it minimizes theoretical complexities and field logistics problems. The configuration that best satisfies these conditions for a hole-to-surface array consists of a buried pole source and a dipole receiver. A current source consisting of a single source pole (current "source") in the drill hole with the other pole (current "sink") located a large distance from the drill hole containing the source, provides the simplest current distribution of the many possible source-sink arrangements. The surface distribution of equipotential lines surrounding a pole source buried in a homogeneous, or one-dimensional layered, half-space is in the form of concentric circles around the buried source pole.

A dipole potential receiver, consisting of closely spaced poles, enables the interpreter to calculate the approximate electric fields. The non-radial components of the electric field are zero in a homogeneous or a laterally isotropic earth. However, when lateral inhomogeneities are present in the geoelectric section, the direction of the electric current emanating from a buried current source is not radial, and it is necessary to measure two orthogonal components of the potential in order to calculate the total electric field measured on the surface. The direction of the total electric field can be computed from orthogonal potential dipole measurements if the signal polarity is known, which can be accomplished by maintaining a consistent orientation of the polarity of the receiver and using an asymmetric square wave source signal.

The source-receiver configuration used in this study is shown in figure 2. The orthogonal potential field measurements were made at stations on a

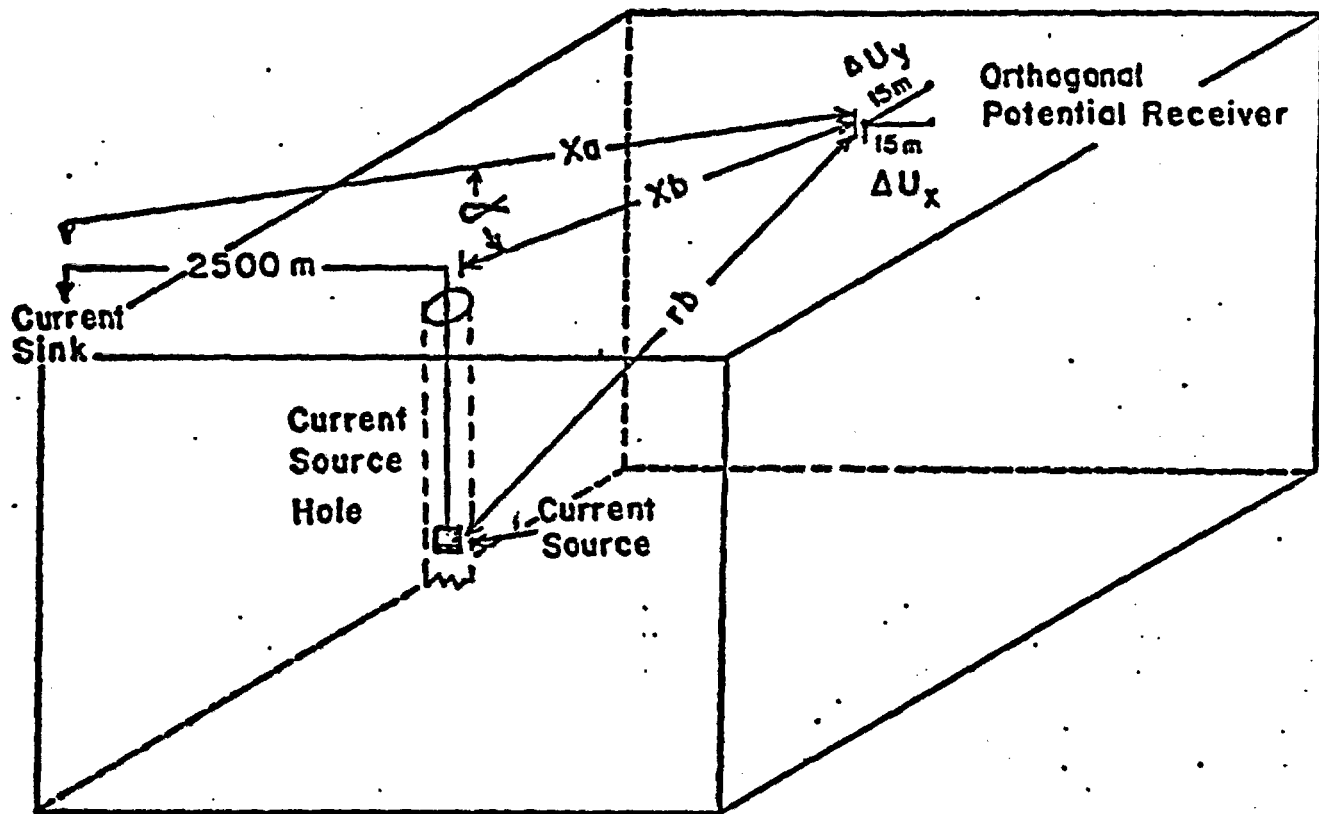


Figure 2.—Field measurement configuration. The total electric field is calculated from the orthogonal dipole potential measurements. ($E_t = ((\Delta U_x/15)^2 + (\Delta U_y/15)^2)^{1/2}$). The distances X_b , r_b , and X_a ($r_a = X_a$) are used in the apparent resistivity calculation.

grid over a area-enclosing drill holes UE25a-4, -5, and -6, making it possible to repeat potential measurements for sources in each of the four drill holes shown in figure 1. Source pole depths for holes UE25a-1, -4, -5, and -6 were 762 m, 149 m, 149 m, and 152 m, respectively.

Reduction and analysis of field data

Contour maps of the magnitude and direction lines of the total electric field are shown in figure 3 for current sources in each of the four drill holes. The magnitude of the surface electric field was calculated using $E_t = (E_x^2 + E_y^2)^{1/2}$, where E_x and E_y are the orthogonal electric field components calculated by dividing the measured dipole potential by the receiver dipole length. The direction of the total electric field was calculated by computing the inverse tangent of the orthogonal electric field components.

Electric field measurements for source holes UE25a-4 and -5 (figures 3(a), and 3(b)) illustrate a generally radial distribution of the direction of the electric field away from the drill hole containing the current source, and a nearly circumferential contour pattern of the magnitude near the source holes.

Concentric contour patterns for the magnitude are not as evident for source holes UE25a-1 and -6 (figures 3(c), and 3(d)). However, the direction lines for holes UE25a-1 and -6 do radiate away from the source holes. The lack of a concentric contour pattern near drill hole UE25a-6 (figure 3(c)) is probably caused by the presence of anomaly "A" in the vicinity of the source. The absence of a concentric contour pattern around the source hole for the electric field with the deep source in drill hole UE25a-1 may indicate

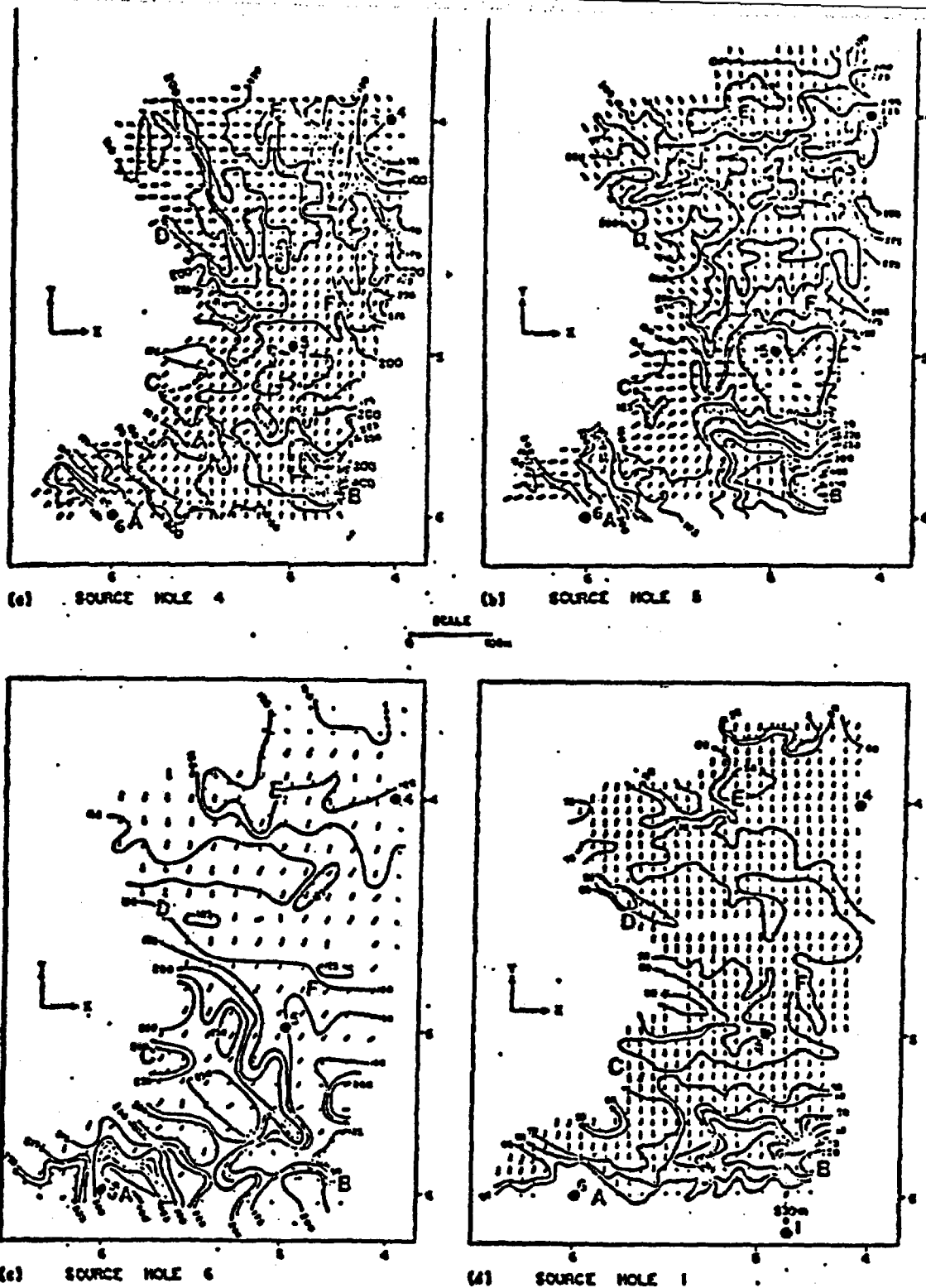


Figure 3.—Contour maps of the magnitude of the normalized total electric field divided by the source current for: (a) the current source in drill hole UE25a-4, (b) the current source in drill hole UE25a-5, (c) the current source in drill hole UE25a-6, and (d) the current source in drill hole UE25a-1. The direction of the total electric field is shown by lines originating at the measurements station locations (indicated by dots "."). Units for (a), (b), and (c) are $V/(A \cdot H)$ multiplied by 10^6 while units for (d) are $V/(A \cdot M)$ multiplied by 10^7 .

the presence of lateral inhomogeneities either at depth, or away from the measurement grid. Two prominent anomalies are located in the lower portions of the contour maps in figure 3. An anomalous increase in the magnitude is present in the vicinity of the region marked "A" for source holes UE25a-4, -5, and -6, and in the vicinity of the region marked "B" for source holes UE25a-1, -4, and -5. The interpretation of these anomalies is discussed at length later in this paper.

The apparent resistivity is calculated from the total electric field using the formula:

$$\rho_a = E_t \left(\frac{2H}{I} \right) \left[\frac{X_a^2}{r_a^6} + \frac{X_b^2}{r_b^6} - \frac{2X_a X_b}{r_a^3 r_b^3} \cos(\alpha) \right]^{-1/2}$$

where I is the input current, r_a is the total distance between the "A" current sink and the receiver, r_b is the total distance between the "B" current source and the receiver, X_a and X_b are the surface projections of r_a and r_b , respectively, and α is the included angle of X_a and X_b . Apparent resistivity contour maps for each of the four source holes are shown in figure 4. The apparent resistivity maps show a circumferential contour pattern for source holes UE25a-4, -5, and -6 (figures 4(a), 4(b), and 4(c)), reflecting the layered nature of the volcanic tuff sequence. The anomaly seen in region A for the electric field contour maps is enhanced by the apparent resistivity calculation for source holes UE25a-4, -5, and -6, but is not markedly affected by the calculation for source hole UE25a-1. The resistivity anomaly in region B is not noticeably affected by the apparent resistivity calculation for any of the source holes. However, resistivity lows in the vicinity of D and E are

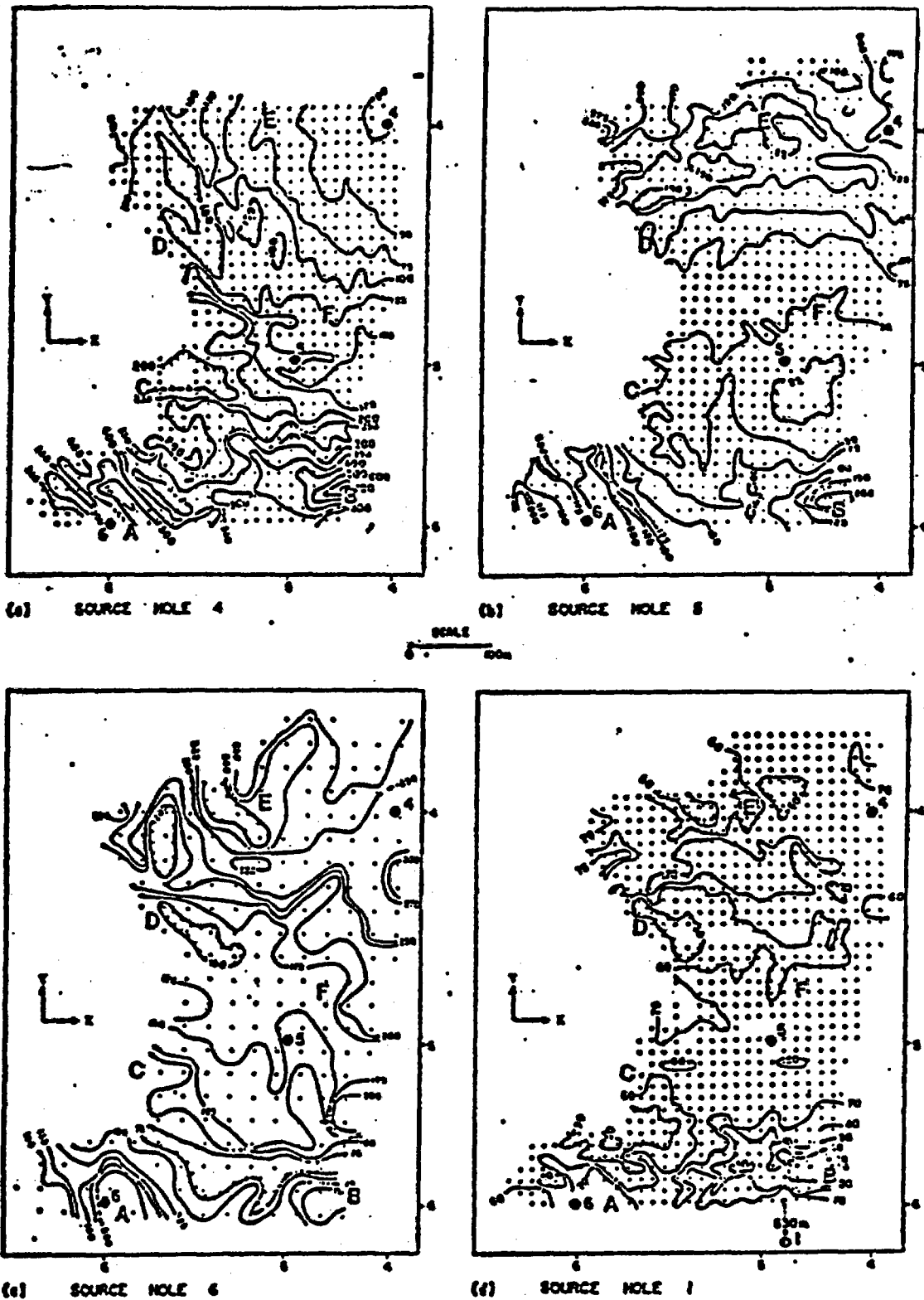


Figure 4.—Contour maps of apparent resistivity (in ohm-m) for: (a) current source in drill hole 4, (b) current source in drill hole UE25a-5, (c) current source in drill hole UE25a-6, and (d) current source in drill hole UE25a-1. The dots indicate the field measurement locations.

enhanced in the circumferential direction to the current source for holes UE25a-4 and -5 (figures 4(a) and 4(b)). These low amplitude resistivity anomalies are more noticeably affected by the apparent resistivity calculation than the higher intensity anomalies (e.g., areas A and B).

Layered-earth reduction of field data

Geophysical well logs and core from each of the drill holes in the study area indicates the presence of a layered stratigraphic and geoelectric section that nearly parallels the topographic dip in the mapped area (Hagstrum and others, 1980; Daniels and others, 1981; Spengler and others, and Spengler and Rosenbaum, 1980). It was noted earlier that the electric field and apparent resistivity maps (figures 3 and 4) also show a generally concentric contour pattern around the current source that is indicative of a layered earth.

Profiles from the resistivity contour maps in figure 4 are shown in figure 5 along with a layered earth model and the corresponding model response for source depths of 137 m (model X, for source holes UE25a-4, -5, and -6) and 762 m (model Y, for source hole UE25a-1). The depth of the interface between layers 4 and 5 is approximately equal to the depth of the water table. A decrease in resistivity near the water table, as indicated by the well logs in hole UE25a-1 (Hagstrum and others, 1980), is necessary to obtain the low apparent resistivity values for the source in hole UE25a-1.

A residual apparent resistivity map is obtained by subtracting the layered earth model response from the field data. Residual maps for the four drill holes discussed in this paper are shown in figure 6. Regions on the residual maps that have values near-zero are zones where the layered earth

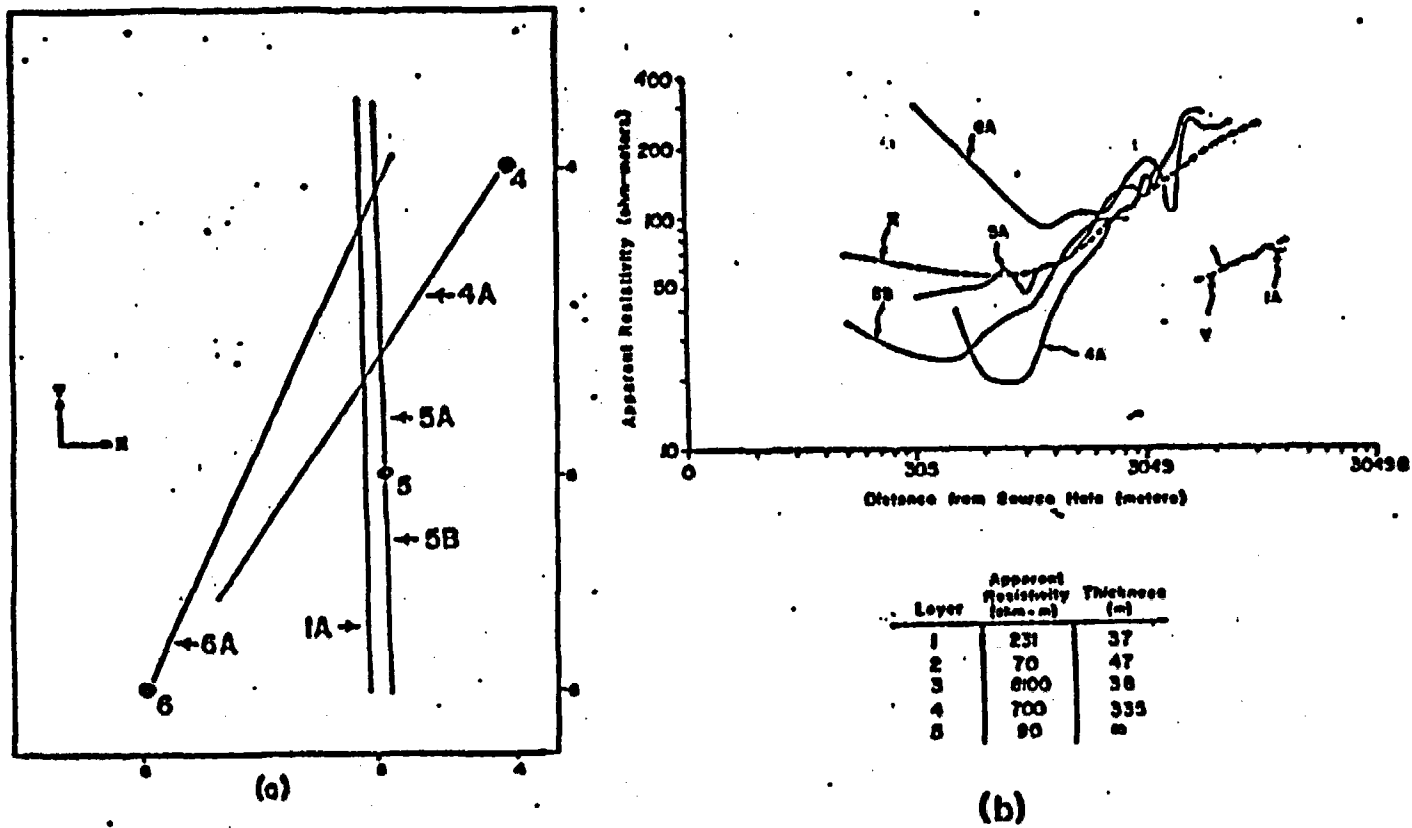


Figure 5.—Apparent resistivity profiles, layered earth model, and model responses. Profile locations are shown in (a), while profile values of field data and model response values are shown in (b).

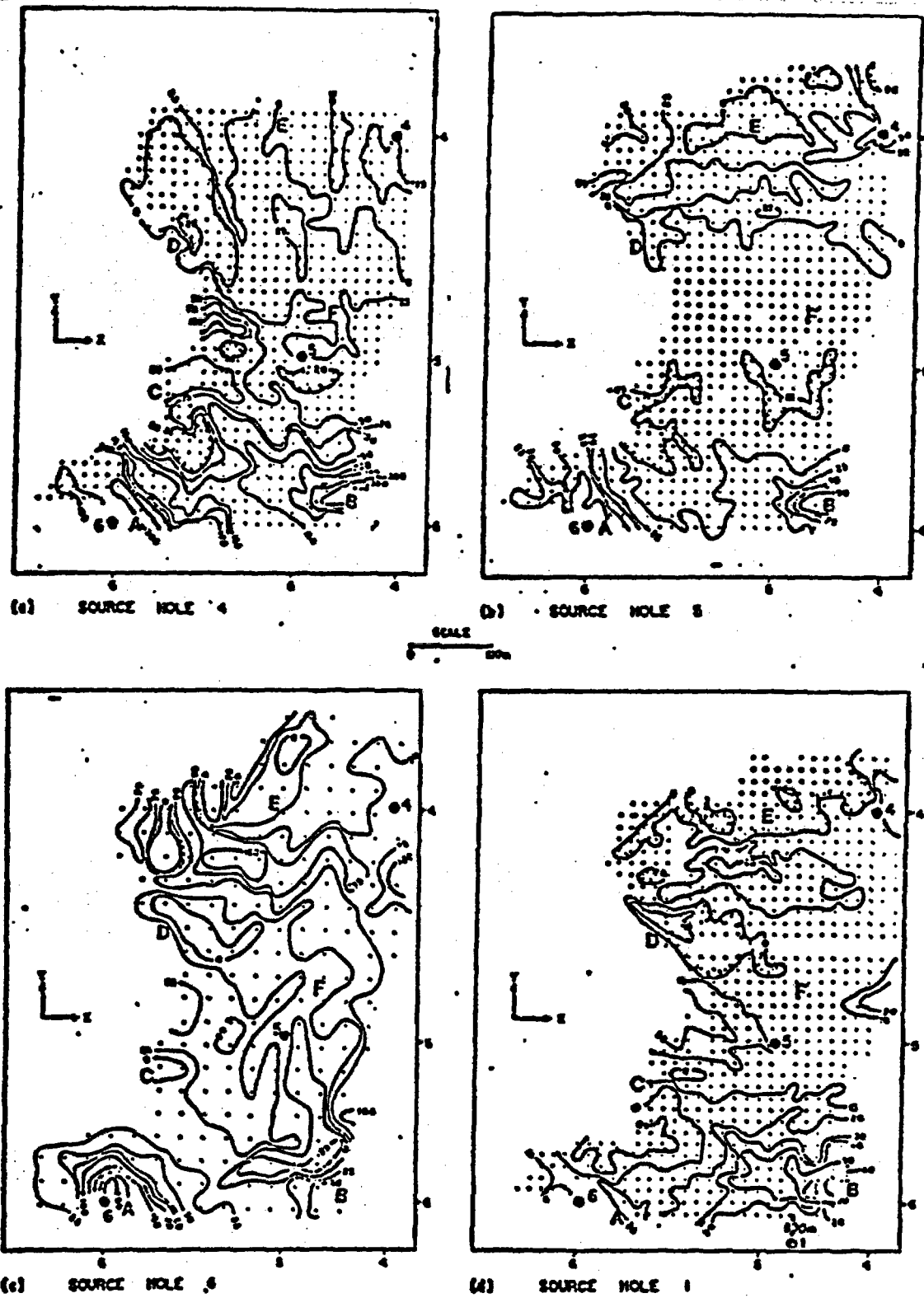


Figure 6.—Residual apparent resistivity contour maps (in ohm-m) for source holes (a) UE25a-4, (b) -5, (c) -6, and (d) -1.

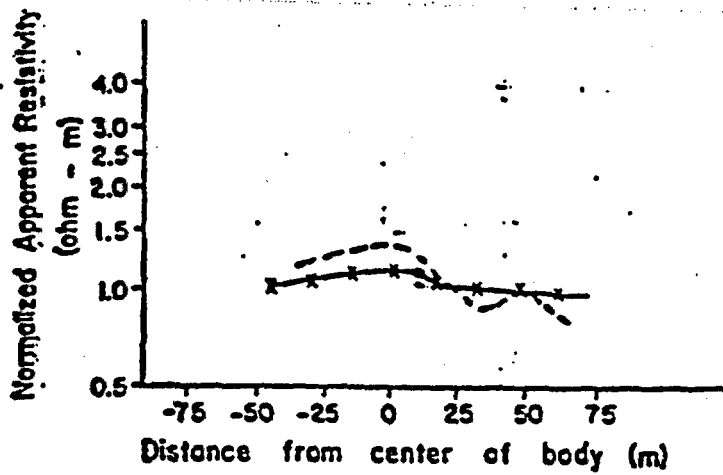
model fits the field data. The most prominent near-zero region on the maps in figure 6 is contained in area F. Regions containing anomalous resistivity anomalies include areas A and B, D and E. Anomalies on the residual maps cannot be interpreted directly with two and three dimensional models because the responses of an inhomogeneity and a layered earth are not additive. However, the residual map serves a useful purpose of qualitatively accentuating the spatial extent of anomalies. The use of multiple source holes and the use of electric field and resistivity maps (figures 3 and 4) makes it possible to confirm the horizontal locations of anomalies on the residual maps and to infer the likely locations and shapes of the bodies causing the anomalies.

Comparison of field data with three dimensional models

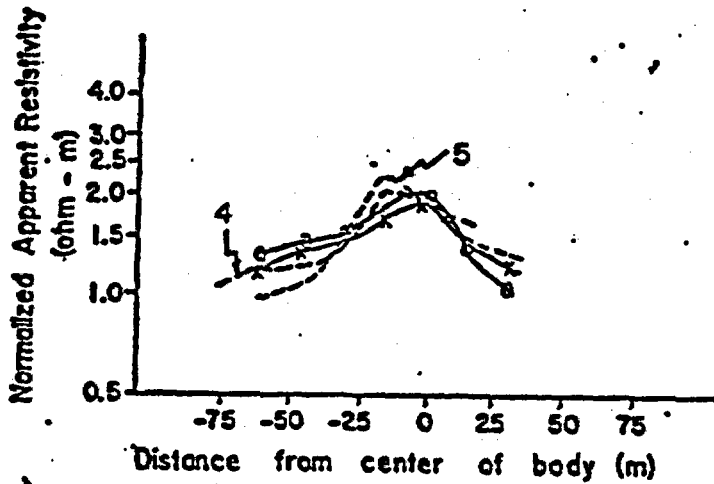
Mathematical models are not commonly available for the resistivity response of three dimensional bodies in a layered earth. Quantitative interpretation of residual anomalies in terms of two or three dimensional bodies, computed as in figure 6, is not valid since the response of a three dimensional body in a layered earth is not simply the additive effect of the layered earth response and the three dimensional body response. However, a qualitative evaluation of individual anomalies can be obtained by comparing the field data with three dimensional models in a homogeneous half-space. The three dimensional models presented in this study were generated using a surface integral technique developed by Barnett (1972) that has been modified for buried electrodes (Daniels, 1977) and for calculating the apparent resistivity from the total electric field. If a fixed resistivity contrast is assumed, then the approximate shape and depth of the anomalous bodies can be estimated

from three dimensional models. A fixed resistivity contrast is used for models presented in this section, even though there is a large resistivity contrast between individual layers.

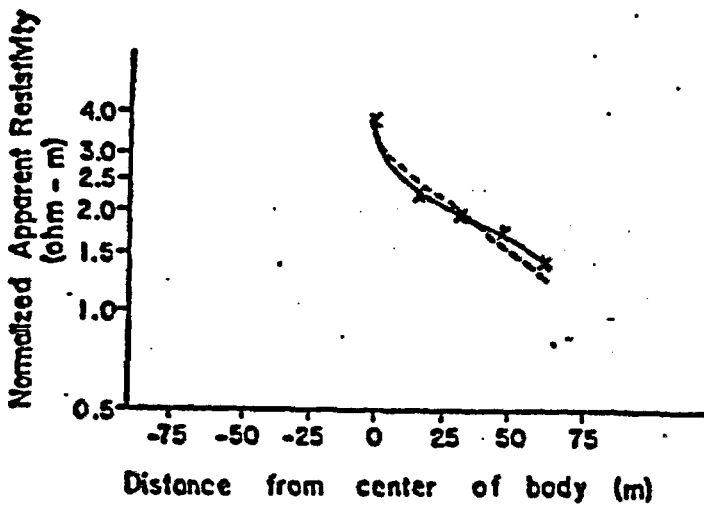
The high resistivity anomaly in the vicinity of zone A (figures 4 and 6) has the following characteristics: (1) the resistivity high is elongated with a steep gradient for source holes UE25a-4 and -5, (2) the anomaly is broader and less elongated for source hole UE25a-6, (3) the amplitude of the anomaly is very low for source hole UE25a-1, and (4) the position of the anomaly is approximately the same for each of the four source holes. Figure 7 shows normalized apparent resistivity responses across a three dimensional, vertical tabular body for source pole positions that are equivalent to the source hole positions with respect to the high resistivity anomaly in area A. These profiles illustrate that a near-surface, vertical tabular body has an apparent resistivity profile that is similar to normalized profiles for the field data. The model response profile for a distance and depth equivalent to source hole UE25a-1 (figure 7(a)) shows a very low amplitude anomaly similar to that seen in the field data. The response when the body is close to the source (figure 7(c)) is similar to that seen for the field data when the source is in drill hole UE25a-6. The model response when the source is the same relative position as for drill holes UE25a-4 and -5 (figure 7(b)) shows a narrow, high amplitude anomaly. There is practically no difference in the model responses for source hole positions UE25a-4 and -5 even though the amplitude of the apparent resistivity for the field data near anomaly "A" is different. The difference in amplitude for the field data is caused by differences in the geoelectric properties near the different source holes rather than specific characteristics of the body causing anomaly A.



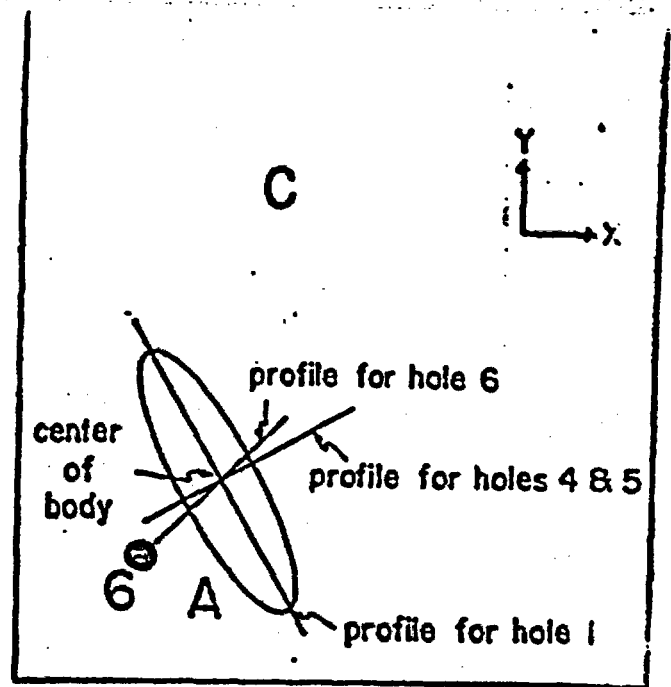
(a) Source hole 1



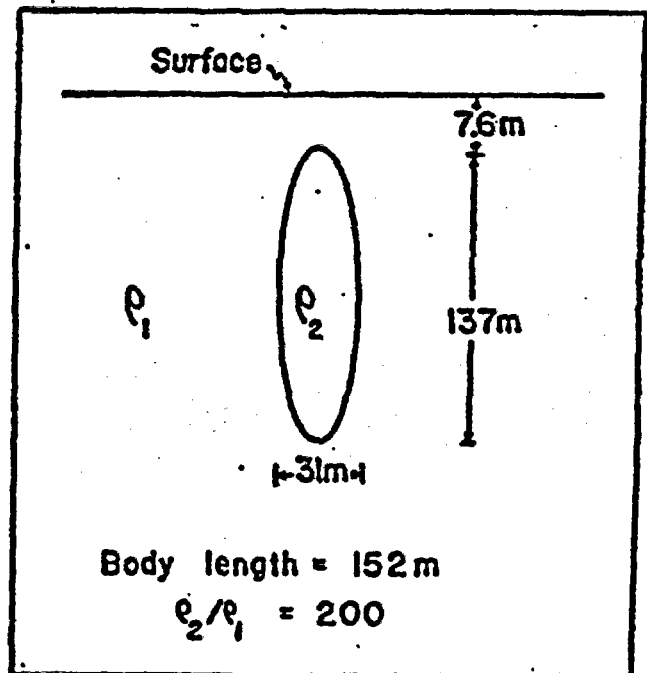
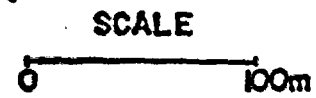
(b) Source holes 4 and 5



(c) Source hole 6.



Plane view: Anomaly A

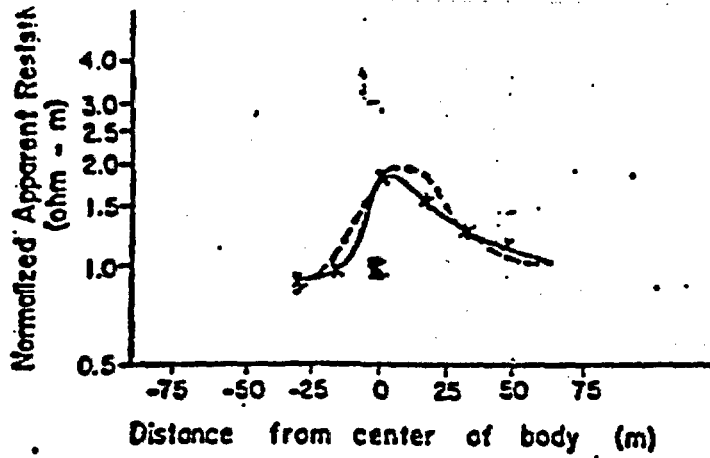


Cross sectional view: Anomaly A

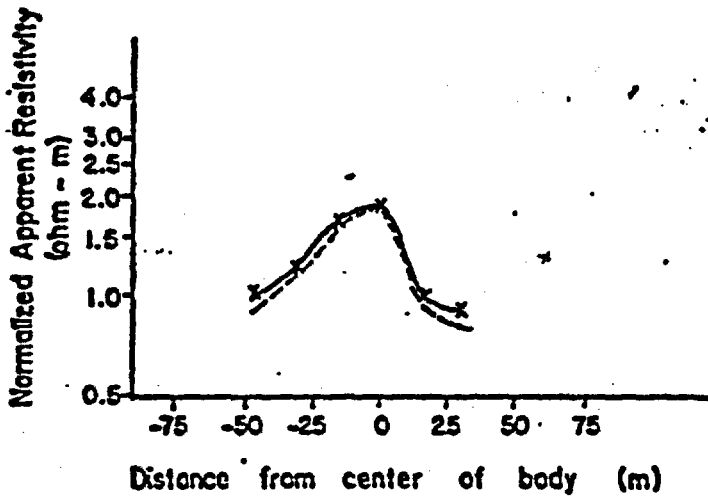
Figure 7.—Normalized apparent resistivity profiles for the high resistivity anomaly in area A for field data (indicated by dashed lines) and model responses for (a) source hole 1, (b) source holes 4 and 5, and (c) source hole 6. The field data for source hole UE25a-1, -4, -5, and -6 are normalized by dividing the field data by 100, 250, ...

The high resistivity anomaly in area B has the following characteristics: (1) the anomaly has a high amplitude and is in the shape of an ellipse for source holes UE25a-1, -4, and -5, (2) the size and amplitude of the anomaly is small for source hole UE25a-6, (3) since the anomaly is centered near the edge of the maps, the actual length of the anomaly is unknown. Model responses for a horizontal lens using source positions equivalent to the field measurement array are shown in figure 8 along with the normalized apparent resistivity field profiles. The amplitude for a near-surface lens is high for source positions equivalent to holes UE25a-1, -4, and -5 (figure 8(a), 8(b) and 8(c), respectively). The lack of a pronounced anomaly in region B for source hole UE25a-6 may be caused by the proximity of source hole to anomaly A, which interferes with the normal flow of electric current away from drill hole UE25a-6.

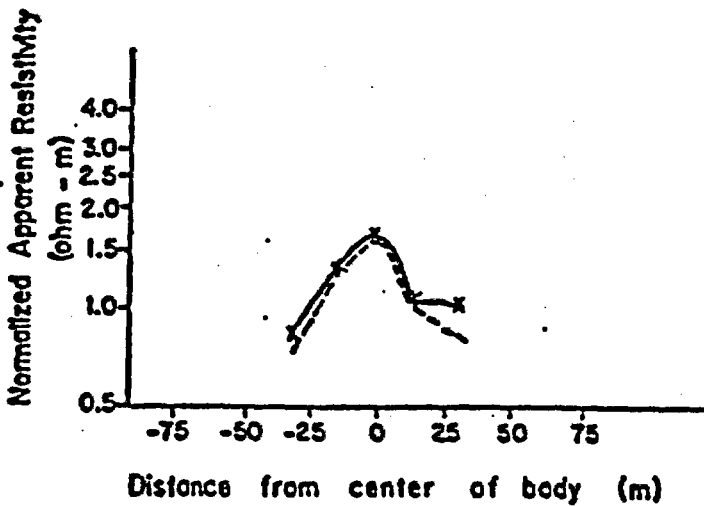
Anomalies shown on the resistivity and residual maps for areas C, D, and E have a lower amplitude than the high resistivity anomalies in areas A and B. A large low resistivity anomaly (negative residual anomaly) is present near area D for source holes UE25a-4 and -6, while low resistivity anomalies trending nearly perpendicular to this anomaly are present for source hole UE25a-1. The shapes of these low amplitude anomalies are variable for each of the source holes. The low amplitude and inconsistent shapes of these anomalies for various sources suggests a low resistivity contrast with the surrounding media. The inconsistent shapes and positions of these anomalies for the different source holes makes it impossible to compare the field data directly with the model responses. However, model responses for shallow three dimensional bodies can provide a general basis for interpreting these



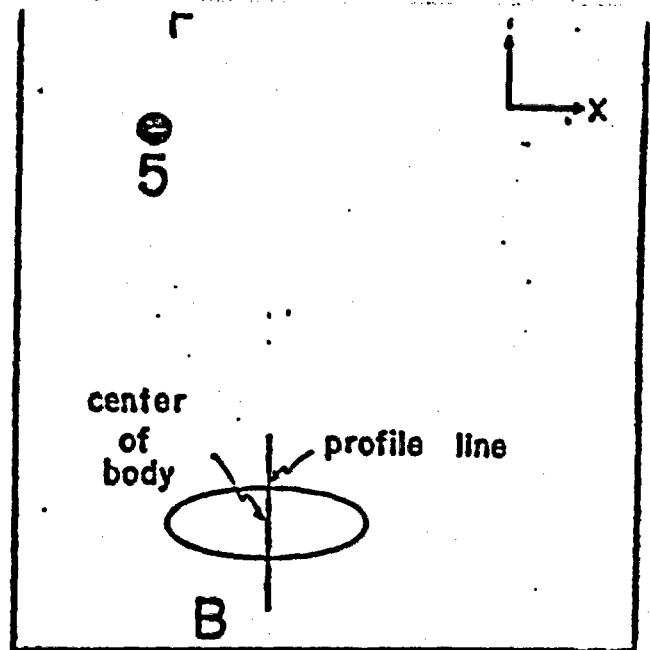
(a) Source hole 1



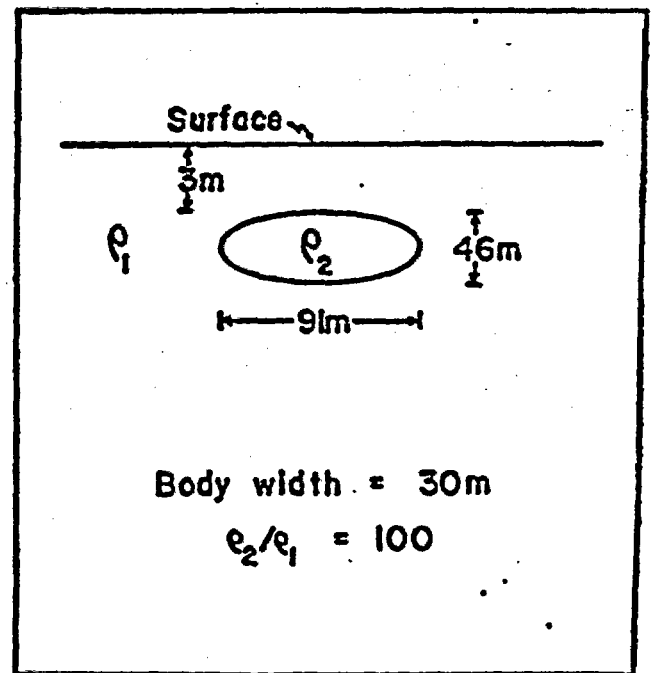
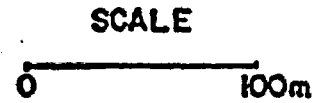
(b) Source hole 4



(c) Source hole 5



Plane view: Anomaly B



Cross sectional view. Anomaly B

Figure 8.—Normalized apparent resistivity profiles for the high resistivity anomaly in area B for field data (indicated by dashed lines) and model responses for (a) source hole 1, (b) source hole 4, and (c) source hole 5. The field data for source holes UH25u-1, -4, and -5 are normalized by dividing the field data by 85, 400, and 150,

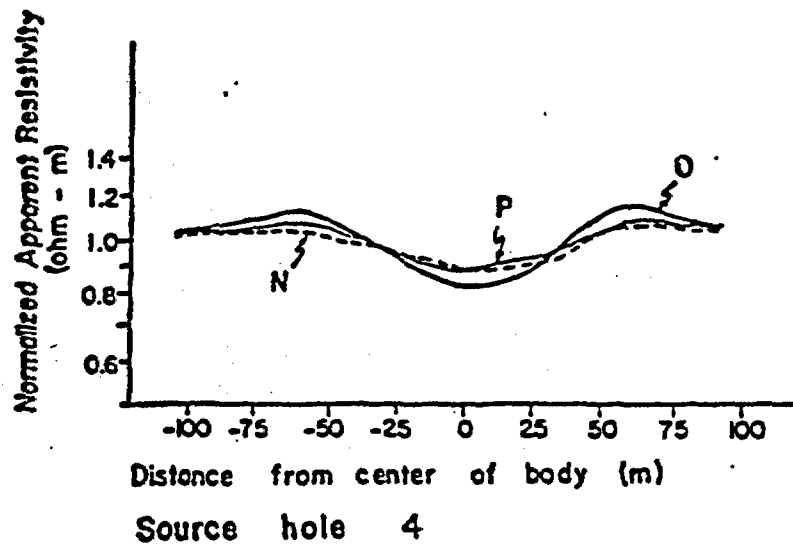
anomalies. Figure 9 illustrates the response of a broad horizontal, lens-shaped conductive body with a low resistivity contrast with the surrounding media. The model responses for a source position equivalent to source hole UE25a-4 (figure 9) suggests that there is only a small change in amplitude as a function of depth and resistivity contrast. The model profiles in figure 9 do not explain the erratic positions of the low resistivity anomalies for the different source holes, suggesting that these anomalies are not due to simple three dimensional bodies.

Summary of data interpretation

The hole-to-surface resistivity data illustrates that the surveyed region can be characterized as representing the following three distinct geoelectric zones: (1) the volume near source hole UE25a-5 (region F) is primarily laterally homogeneous and layered, (2) regions A and B contain high amplitude resistivity anomalies that may reflect resistive bodies in the layered section, and (3) regions C, D, and E contain a complex pattern of low amplitude anomalies.

The fixed position and similar shapes for the different source holes suggests a near surface geologic source for the anomalies in regions A and B. The high resistivity linear anomaly in region A may be representative of a calcified or silicified fracture zone, while elliptically-shaped high amplitude anomaly in region B may be caused by a near-surface devitrified, lithophysal zone which are known to be present in the area.

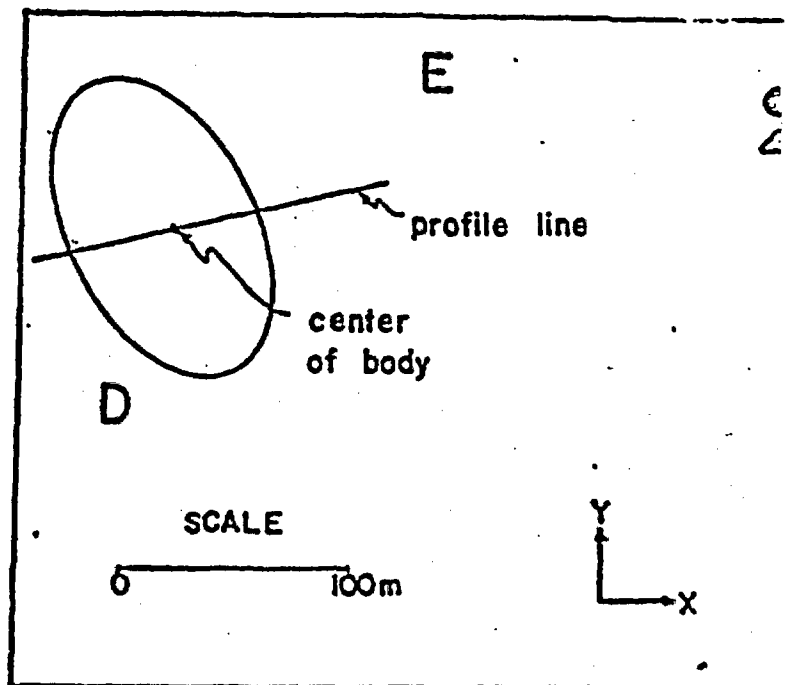
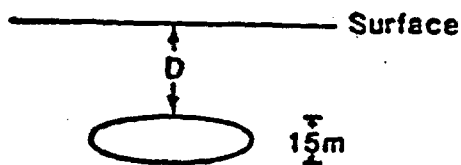
Regions D and E enclose high and low resistivity anomalies of varying shapes and trends. These regions are located in close proximity to the



Explanation:

Profile	Equivalent Source Hole	D	$\rho_2 : \rho_1$
N	4	23	1:3
O	4	8	1:3
P	4	8	1:2

Cross Section of Ellipsoid



Plane view:

Figure 9.—Normalized apparent resistivity profile for the low resistivity anomaly (negative residual anomaly).

intersection of a secondary easterly-trending valley (near the 1311 contour designation in figure 1), and the valley in which the measurements were made. This area of intersection of the valleys could cause localized thickening of alluvial material, resulting in low amplitude resistivity anomalies. Three dimensional models also suggest a shallow source for the low resistivity anomalies. However, the erratic positions of the low resistivity anomalies for the different source holes suggests that these anomalies are not due to simple three dimensional bodies, but may be caused by a complex combination of interfering effects related to variations in alluvium thickness.

Conclusions

Field data and models presented in this study illustrate the use of hole-to-surface resistivity measurements for defining geoelectric inhomogeneities. The utility of hole-to-surface direct current field data can be enhanced by making total electric-field measurements over a closely spaced grid on the surface. Verification of the presence of anomalies is improved by repeating measurements from several different source holes in an area. Repeating measurements from several source holes also helps when interpreting data for a single current source that may be located in an anomalous geoelectric zone.

Modeling can aid the qualitative interpretation of hole-to-surface resistivity data. Residual anomaly maps, calculated by subtracting a layered earth model response from the field data, can help to isolate anomalous areas within layered areas. The qualitative aspects of anomalous bodies can be determined by three dimensional modeling.

Hole-to-surface resistivity measurements at Yucca Mountain indicate the presence of near-surface resistive anomalies near drill holes UE25a-6, and UE25a-1. The resistive anomaly near drill hole UE25a-6 indicates the presence of a thin, vertical, resistive body that nearly intersects the surface, while the anomaly near UE25a-7 is probably caused by a horizontal lens-shaped body that is also near the surface. Many conductive anomalies were detected to the west of UE25a-4. However, it is likely that these anomalies are caused by variations in the thickness of the surface alluviums.

References

- Alfano, Luigi, 1962, Geoelectrical prospecting with underground electrodes: *Geophys. Prosp.*, v. 10, no. 3, p. 290-303.
- Barnett, C. T., 1972, Theoretical modeling of induced polarization effects due to arbitrarily shaped bodies: Colorado School of Mines, Ph. D. Thesis.
- Daniels, J. J., 1977, Three dimensional resistivity and induced polarization modeling using buried electrodes: *Geophysics*, v. 42, no. 5, p. 1006-1019.
- Daniels, J. J., 1978, Interpretation of buried electrode resistivity data using a layered earth model: *Geophysics*, v. 43, no. 5, p. 988-1001.
- Daniels, J. J., Scott, J. E., and Hagstrum, J. T., 1981, Interpretation of geophysical well log measurements in drill holes UE25a-4, -5, -6, and -7, Yucca Mountain, Nevada Test Site: U.S. Geological Survey Open-File Report 81-615.
- Hagstrum, J. T., Daniels, J. J., and Scott, J. E., 1980, Interpretation of geophysical well log measurements in drill hole UE25a-1, Nevada Test Site, Radioactive Waste Program: U.S. Geological Survey Open-File Report 80-941.
- Merkel, R. H., and Alexander, S. S., 1971, Resistivity analysis for models of a sphere in a halfspace with buried current sources: *Geophys. Prosp.*, v. 19, no. 4, p. 640-651.
- Snyder, D. D., and Merkel, R. M., 1973, Analytic models for the interpretation of electrical surveys using buried current electrodes: *Geophysics*, v. 38, p. 513-529.

Spengler, R. W., and Rosenbaum, J. G., 1980, Preliminary interpretations of geologic results obtained from boreholes UE25a-4, -5, -6, and -7, Yucca Mountain, Nevada Test Site: U.S. Geological Survey Open-File Report 80-929.

Spengler, R. W., Muller, D. C., and Livermore, R. B., 1979, Preliminary report on the geology and geophysics of drill hole UE25a-1, Yucca Mountain, Nevada Test Site: U.S. Geological Survey Open-File Report 79-1244.